Antideuteron Production in High Energy Heavy Ion Collisions

J. L. Nagle, B. S. Kumar, M. J. Bennett, S. D. Coe, G. E. Diebold, and J. K. Pope
A.W. Wright Nuclear Structure Laboratory, Yale University, New Haven, Connecticut 06520-8124

A. Jahns and H. Sorge
Institut für Theoretische Physik 60054 Frankfurt am Main 11, Germany
(Received 18 April 1994)

Experiment E858 at the Brookhaven National Laboratory Alternating Gradient Synchrotron has recently reported the detection of two antideuterons produced in 14.6A GeV/c Si + Au collisions. The data were interpreted as implying antideuteron production rates about an order of magnitude below expectations. We use an extended RQMD model to demonstrate that the antideuteron yields are readily explained in a dynamical scenario that includes collective expansion and strong antinucleon absorption.

PACS numbers: 25.75.+r

The enhanced production of antibaryons has been proposed as a potential signature for the identification of a novel state of matter: the quark-gluon plasma [1]. Heavy ion collisions at energies of the BNL Alternating Gradient Snychrotron (AGS) (10–15 GeV per nucleon) have been used to create nuclear matter at high baryon density (about 6 to 10 times normal nuclear matter density), and, possibly, quark matter [2]. Any enhanced production of antiprotons ($\overline{p}$) and antideuterons ($\overline{d}$) may be counterbalanced by annihilation in this unusual environment. Antibaryon distributions could therefore be both a signature for quark matter formation and a probe of this baryon density [3]. There are two models, RQMD [4] and ARC [5], that have successfully described antiproton spectra for Si beams at AGS energies. In the RQMD model, the initial production and the subsequent annihilation of the antiprotons is large. In the ARC model, fewer antiprotons are initially produced, but $\overline{p}$ annihilation is "screened" in the high density collision environment. Any effect of the collision environment on the production and annihilation of antiprotons will be further enhanced in the production and annihilation of antideuterons. It is therefore important to understand how and how often antinuclei (and in particular the $\overline{d}$) are produced.

The first reported measurement of the $\overline{d}$ [6] was able to account for the yields in p + Cu collisions in terms of a "simple" coalescence model. The measurement of antideuterons in experiment E858 at the BNL AGS has been interpreted similarly [7,8] and represents an unexpectedly low yield when compared to the predictions of simple coalescence models. This result may provide information on hadronization and annihilation processes in baryon rich environments and also shed light on a possible screening of the annihilation of antiprotons [5] and antideuterons. Thus, it is important to better understand the E858 result and possible shortcomings in the coalescence models used in its analysis.

First, we discuss coalescence models, the specific assumptions they make, and whether these assumptions are consistent with experimental data. The simple coalescence picture, first put forth by Butler and Pearson [9] and later extended by Schwarzschild and Zupančič [10], describes the invariant cross sections of light nuclei with atomic number A in terms of a scale factor and the Ath power of the proton invariant cross sections [11]. The same equation when cast in terms of invariant multiplicities [8] yields a scale factor B_A which should be unique for a given nuclear species and should not vary with beam energy, target, and projectile mass. Also, one would expect B_A to have the same value for a nucleus and its antinucleus. We use $\overline{B_A}$ for clarity to describe the same quantity for antinuclei. The B_A values obtained for light nuclei from numerous LBL Bevalac experiments studying nucleus-nucleus collisions [12] and CERN Super Proton Sychrotron (SPS) [13] and Fermilab [14] experiments studying p + A collisions seem to be relatively independent of energy, as is shown in Fig. 1. There is no Bevalac data for antideuterons. However, as also shown in the

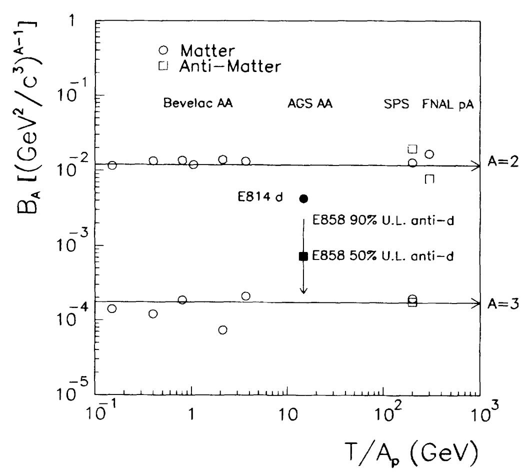

FIG. 1. Coalescence scaling factor B_A for matter and antimatter plotted as a function of the kinetic energy per nucleon T/A (GeV). The data for nuclei are from [12–14] and the data for the antinuclei are from [7,8,13,14].

same figure, data from $p + A$ collisions at higher energies yield scaling factors for antinuclei which are similar to those for nuclei.

The above data are in reasonable agreement with the simple coalescence model. However, this model calculates the production of the (anti)deuteron by considering the proximity of the (anti)nucleons in momentum space only and ignores their spatial separations, at the times when the (anti)nucleons have stopped interacting (at freeze-out). In reality, greater spatial separation between nucleons at freeze-out lowers the probability for the formation of heavier nuclei. Thus, one would expect the scale factor (B_A) to be inversely related to the average separation between the nucleons at freeze-out and there from the volume of the system. If all the nucleons are within a small volume of the size of the deuteron (rms diam = 4.2 fm), then the spatial overlap factor can be ignored and B_A should be constant. Although projectiles of mass as large as $A = 40$ were used at the LBL Bevalac, few secondary particles are produced due to the low beam energy. Thus, the collision volume does not appear to expand significantly before freeze-out. All the data at higher energies (greater than $200A$ GeV/c) from SPS and Fermilab are for $p + A$ systems. These collisons, therefore, have small interaction volumes despite the significantly higher energy. For collision volumes with dimensions far in excess of that of the deuteron, the simple coalescence model fails (B_A is not a constant), as we discuss below.

Also shown in Fig. 1 is the value for $\overline{B_2}$ measured by experiment E858 for antideuterons at $p_t = 0$ produced in minimum bias $14.6A$ GeV/c Si + Au interactions [8]. The value is significantly lower than previously seen in the $p + A$ data and inconsistent with the simple coalescence description.

In the attempts to understand the E858 measurement, comparisons were made between the scaling factor for deuterons and antideuterons, at a time when no published scaling factors for deuterons at AGS energies were available. Thus, B_2 measured at the Bevalac was compared to $\overline{B_2}$ measured at the AGS [7,15]. Recently, AGS experiment E814 has reported the deuteron scaling factor at $p_t = 0$ in minimum bias Si + Pb collisions to be $B_2 = (4.3 \pm 0.2) \times 10^{-3}$ [16,17]. These data are also shown in Fig. 1 and are significantly lower than the Bevalac B_2 value used in previous attempts to understand the E858 data. It is important to note that although B_2 and $\overline{B_2}$ at AGS energies are not equal within uncertainties, both values are below the Bevalac and higher energy $p + A$ experimental results.

Deviations from the simple coalescence model are more striking if one looks at the collision geometry dependence of B_A. Data from experiment E814 for Si + Pb at $14.6A$ GeV/c reveal a significantly lower value for B_2 for deuterons produced in central collisions than in peripheral collisions by a factor of approximately 40 [16,17].

The decrease in B_2 for the AGS data can be understood in the context of the thermodynamic [18] and density matrix models [19] as implying a freeze-out volume and radius that are large in comparison to those of the deuteron. An RMS radius has been deduced for central Si + Pb collisions, using a density matrix model, to be 7.1 fm [17], indicating substantial expansion of the system beyond the sizes of the colliding nuclei. In contrast, there appears to be minimal expansion of the collision volume at the lower Bevalac energies and in $p + A$ collisions at higher energies. Although the density matrix and thermodynamics models can explain the variations in B_A, they are inadequate for a detailed description of the AGS $\overline{d}$ and d data [8,17]. Both models assume that the source of (anti)nucleons can be described by a Gaussian distribution, that all nucleons have a common freeze-out time, and that there is no correlation between the positions and momenta of the various (anti)nucleons. All of the above are inaccurate [20,21]. In an attempt to reconcile the E858 data, it has been pointed out that, due to the large annihilation cross section of antinucleons in the baryon dense collision environment, the antideuterons may be formed only on the surface of the collision volume and thus not have a Gaussian spatial distribution [15]. In contrast, the nucleons and thus the nuclei would occupy the entire collision volume. Since B_A has been shown to depend on collision geometry [16,17], one can expect this to be reflected in the dependence of B_A and $\overline{B_A}$ for the d and the $\overline{d}$ on projectile, target, and centrality. It is therefore imprudent to make predictions for the $\overline{d}$ yields in E858 based on the B_2 value measured by E814 in minimum bias collisions. Any similarity between $\overline{B_2}$ and B_2 for the minimum bias AGS data could be obscuring some interesting physics which cannot be understood in the framework of the simple coalescence and thermodynamic models. Though there have been improvements to the density matrix model [22] such calculations do not adequately describe the space-time development of the collision volume. We have therefore used a cascade model to study the dynamics of $\overline{d}$ production.

The relativistic quantum molecular dynamics model (RQMD Version 1.07) [23] has been used extensively to describe the spectra of particles, in particular the $\overline{p}$ [4] over a wide range of bombarding energies for several projectile-target combinations. The method of relativistic constraint Hamiltonian dynamics is used to model the nucleus-nucleus collisions at a microscopic level. Models such as RQMD do not include the production of light (anti)nuclei, thus such a calculation must be added as an extension. The previous attempts to calculate deuteron production have employed θ functions with phenomenological parameters in momentum and configuration space [20,24]. The phase space output of RQMD gives the final momenta and locations at which particles suffer their last interactions (defined for an energy threshold of 2 MeV). We consider neutrons and protons in pairs, and if in their center of mass frame they are within $\Delta R = |\vec{r}_1 - \vec{r}_2| = 3.8$ fm and $\Delta P = |\vec{p}_1 - \vec{p}_2| = 185$ MeV/c of each other, we assume they will form a deuteron [20]. Alternatively, we calculate the deuteron formation probability by projecting the nucleon pair phase space on the deuteron wave function via the Wigner-function method as described elsewhere [25]. The deuteron Wigner density (ρ_d^W) is approximated to be that of the ground-state harmonic oscillator wave function. The yield of deuterons is given as

$$dN_d = \frac{1}{2}\frac{3}{4}\left\langle \sum_{i,j} \rho_d^W(\Delta R, \Delta P)\right\rangle d^3(p_{ip} + p_{jn}) \,.$$

The sum goes over all possible n and p pairs, whose relative distance (ΔR) and relative momentum (ΔP) are calculated in the two-nucleon rest frame at a common time after both nucleons have ceased to interact. The factors $\frac{3}{4}$ and $\frac{1}{2}$ account for the n,p pair being in the right spin ($s = 1$) and isospin ($I = 0$) state, assuming no dynamical isospin correlation [21]. We describe details of the Wigner function technique and its application to the description of deuteron production in $p + A$ and $A + A$ collisions elsewhere [26].

The fusion of a neutron and proton into a deuteron has to involve (at least) one additional particle in order to conserve energy and momentum. A coalescence procedure using θ functions does not specify the exact coalescence process and thus retains generality at the expense of having two phenomenological parameters. The process modeled here ($p + n \longrightarrow d$) does not conserve the sum of the free single nucleon energies before fusion. Note, however, that the deuteron binding energy is small (2.3 MeV). Furthermore, the single particle energy spreading just prior to coalescence, which is required from the quantum uncertainty principle, would dominate this energy mismatch [27]. An obvious advantage of the wave function method is its parameter free description of cluster formation [25]. Shown in Fig. 2 are comparisons of the RQMD/coalescence (RQMD/C) calculations with E814 data at $p_t = 0$ for central and minimum bias collisions. The agreement of the calculation with the data for the deuteron system gives us confidence in the coalescence methods and the phase space distribution of nucleons in RQMD. Thus, we apply similar methods to the $\bar{d}$ system.

For the coalescence calculation to be believable, the RQMD prediction for the constituents must be accurate. Shown in Fig. 3 are data for antiprotons measured by experiment E858 in Si + Au collisions at $p_t = 0$ (shown with systematic errors of 20%) [8,28]. Also shown are data from experiments E814 [29] and E886 [30]. The agreement between the experiments and RQMD is reasonable, though the RQMD predictions are low at midrapidity. The calculations do not account for Coulomb forces and do not include the $\bar{p}$ resulting from antilambda ($\bar{\Lambda}$) decay, whose contribution could raise the total $\bar{p}$ yield. Further, it is not clear to what degree the experimental $\bar{p}$ data include contributions from $\bar{\Lambda}$ decay. However, the contribution to the $\bar{d}$ yield from such antiprotons should be negligible because the lifetime of the $\bar{\Lambda}$ (2.631×10^{-10} s) is much longer than the lifetime of the system. Thus the $\bar{p}$ resulting from such decays will be spatially isolated from other antinucleons at that late time. For lack of experimental data, we assume that the $\bar{n}$ distributions are also predicted correctly.

We show in Fig. 3 the $\bar{d}$ distribution calculated using the Wigner density method and the E858 measurement

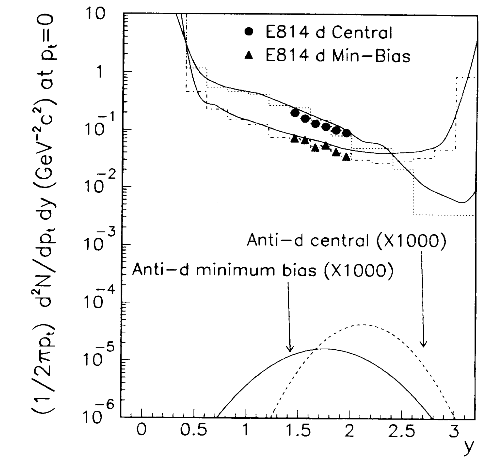

FIG. 2. Deuteron invariant multiplicities measured at $p_t = 0$ by experiment E814 for Si + Pb central and minimum bias collisions [16,17]. Also shown are the RQMD/C calculations for d and $\bar{d}$ ($\times 1000$) for the same centrality cuts. For the d, the histograms and curves are the results of phenomenological and Wigner density calculations, respectively. Both curves for the $\bar{d}$ were calculated using the Wigner density technique.

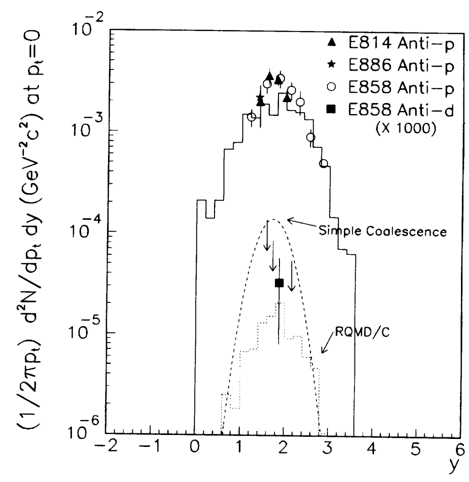

FIG. 3. $\bar{p}$ [7,8,28–30] and $\bar{d}$ [7,8] invariant multiplicities measured at $p_t = 0$ for Si + Au(Pb,Pt) minimum bias collisions at 14.6A GeV/c. Also shown are sensitivity limits for antideuterons where candidates were not observed. The RQMD ($\bar{p}$) and RQMD/C ($\bar{d}$) results are shown as histograms. We also show the results of a simple $\bar{d}$ coalescence calculation as was done previously [7,8].

and upper limits. Additionally, the prediction of the simple coalescence model using the $\overline{p}$ data and the B_2 value from Bevalac data is shown (as was calculated in [7]). The agreement of the RQMD/C prediction with the data reconciles the puzzle of low $\overline{d}$ yields.

We have examined the phase space distributions of the ingredients of antideuterons at the time of last interaction in the RQMD/C model as we have done for deuterons [20]. In Si + Au minimum bias collisions, the $\overline{d}$ distribution is peaked at approximately midrapidity ($y_{NN} = 1.7$) as shown in Fig. 2. However, in central collisions, the mean shifts by almost 0.5 unit of rapidity toward the Si projectile rapidity. This shift is caused by significant annihilation of the antideuterons in the more baryon rich regions of lower (toward Au target) rapidity. Also, in Si + Au central collisions, we have looked at the spatial distribution of the $\overline{d}$ and found a lower density of antideuterons in the very center, suggesting the importance of annihilation. Also, the $\overline{d}$ distribution is distinctly asymmetric. There are fewer antideuterons in the spatial region corresponding to the Au nucleus and more in the region of the Si nucleus, again due to annihilation. In contrast, the d spatial distribution appears to be enhanced in the region of the Au nucleus, as expected.

Although the agreement of RQMD/C with experiment E858 is good, due to the limited data one cannot conclude that RQMD is modeling exactly the space-time distributions of antinucleons and antinuclei. Many of the effects we have discussed above should be more pronounced in the larger Au + Au system. Also, in order to better use the information from light (anti)nuclei production to understand the collision volume and thus the baryon density at freeze-out, centrality information is crucial. We hope such data will soon be available from experiment E864 and will provide additional tests of our calculations.

We have used the RQMD/coalescence model to calculate d and $\overline{d}$ production in nucleus-nucleus collisions. We find that this dynamical model which takes into account collective expansion, strong antinucleon absorption, and coalescence is able to describe the data of experiment E858. We have highlighted very interesting differences between the sources of deuterons and antideuterons. Such differences warrant further theoretical and experimental investigation using both this and other techniques.

This work was supported in part by Grant No. DE-FG02-91ER-40609 with the U.S. Department of Energy.

[1] T. DeGrand, Phys. Rev. D **30**, 2001 (1984).
[2] H. Sorge, Nucl. Phys. **A566**, 633c (1994).
[3] S. Gavin, M. Gyulassy, M. Plumer, and R. Venugopalan, Phys. Lett. **B 234**, 175 (1990).
[4] A. Jahns *et al.*, Phys. Rev. Lett. **68**, 2895 (1992); Nucl. Phys. **A566**, 483c (1994); University of Frankfurt, UFTP Report No. 348/1993.
[5] S. Kahana, Y. Pang, T. Schlagel, and C. Dover, Phys. Rev. C **47**, R1356 (1993).
[6] D.E. Dorfan *et al.*, Phys. Rev. Lett. **14**, 1003 (1965).
[7] A. Aoki *et al.*, Phys. Rev. Lett. **69**, 2345 (1992).
[8] P. Stankus *et al.*, in *Heavy Ion Physics at the AGS*, Report No. MITLNS-2158, 1993, p. 134; Nucl. Phys. **A544**, 603c (1992); P. Stankus, Ph.D. thesis, Columbia University, 1993.
[9] S.T. Butler and C.A. Pearson, Phys. Rev. Lett. **7**, 69 (1961); Phys. Rev. **129**, 836 (1963).
[10] A. Schwarzschild and C. Zupančič, Phys. Rev. **129**, 854 (1963).
[11] L. Csernai and J. Kapusta, Phys. Rep. **131**, 223 (1986).
[12] S. Nagamiya *et al.*, Phys. Rev. C **24**, 971 (1981); R.L. Auble, Phys. Rev. C **28**, 1559 (1983); P. Lemaire, Phys. Rev. Lett. **37**, 667 (1976); M. Anikina, JINR Report No. 1-84-216, Dubna, 1984.
[13] W. Bozzoli, Nucl. Phys. **B144**, 317 (1978).
[14] J.W. Cronin *et al.*, Phys. Rev. D **11**, 3105 (1975).
[15] S. Mrowczynski, Phys. Lett. **B 308**, 216 (1993).
[16] J. Germani, Ph.D. thesis, Yale University, 1993.
[17] J. Barrette *et al.*, Phys. Rev. C **50**, 1077 (1994).
[18] S. Das Gupta and A.Z. Mekjian, Phys. Rep. **72**, 131 (1981).
[19] H. Sato and K. Yazaki, Phys. Lett. **98B**, 153 (1981).
[20] J.L. Nagle *et al.*, Phys. Rev. Lett. **73**, 1219 (1994).
[21] R. Mattiello *et al.*, University of Frankfurt, UFTP Report No. 352/1994.
[22] S. Mroczyinski, Phys. Lett. **B 277**, 43 (1992); P. Danielewicz and P. Schuck, Phys. Lett. **B 274**, 268 (1994); V.L. Lyuboshits, Sov. J. Nucl. Phys. **48**, 956 (1988).
[23] H. Sorge, H. Stöcker, and W. Greiner, Ann. Phys. (N.Y.) **192**, 266 (1989).
[24] C. Dover *et al.*, BNL Internal Report No. BNL-48594; in *Heavy Ion Physics at the AGS*, Report No. MITLNS-2158, 1993, p. 213; A.J. Baltz *et al.*, Phys. Lett. **B 325**, 7 (1994).
[25] M. Gyulassy, K. Frankel, and E.A. Remler, Nucl. Phys. **A402**, 596 (1983).
[26] J.L. Nagle *et al.*, Yale University Report No. 40609-1160 (to be published).
[27] S. Mroczynski, J. Phys. G **13**, 1089 (1987).
[28] B.S. Kumar *et al.*, Nucl. Phys. **A566**, 439c (1994).
[29] J. Barrette *et al.*, Phys. Rev. Lett. **70**, 1763 (1993).
[30] G.E. Diebold *et al.*, Phys. Rev. C **48**, 2984 (1993).